Tetrahedron 65 (2009) 7474–7481

Contents lists available at ScienceDirect

Tetrahedron

journal homepage: www.elsevier.com/locate/tet

Supported palladium catalysis using a heteroleptic 2-methylthiomethylpyridine–*N*,*S*–donor motif for Mizoroki–Heck and Suzuki–Miyaura coupling, including continuous organic monolith in capillary microscale flow-through mode

Roderick C. Jones [a,*], Allan J. Canty [a,*], Jeremy A. Deverell [a,b], Michael G. Gardiner [a], Rosanne M. Guijt [b], Thomas Rodemann [c], Jason A. Smith [a], Vicki-Anne Tolhurst [a]

[a] School of Chemistry, University of Tasmania, Private Bag 75, Hobart TAS 7001, Australia
[b] Australian Centre for Research on Separation Science (ACROSS), Private Bag 75, Hobart TAS 7001, Australia
[c] Central Science Laboratory (CSL), University of Tasmania, Private Bag 74, Hobart TAS 7001, Australia

ARTICLE INFO

Article history:
Received 16 April 2009
Received in revised form 24 June 2009
Accepted 2 July 2009
Available online 8 July 2009

Keywords:
Catalysis
Supported catalysis
Monolith
Flow-through microreactor
Pyridine
Methylthiomethylpyridine

ABSTRACT

Flow-through catalysis utilising (2-methylthiomethylpyridine)palladium(II) chloride species covalently attached to a macroporous continuous organic polymer monolith synthesised within fused silica capillaries of internal diameter 250 μm is described, together with related studies of ground bulk monolith compared with supported catalysis on Merrifield and Wang beads and homogeneous catalysis under identical conditions to bulk supported catalysis. The monolith substrate, poly(chloromethylstyrene-*co*-divinylbenzene), has a backbone directly related to Merrifield and Wang resins. The homogeneous precatalyst $PdCl_2(L^2)$ (L^2=4-(4-benzyloxyphenyl)-2-methylthiomethylpyridine) contains the benzyloxyphenyl group on its periphery as a model for the spacer between the '$PdCl_2$(N∼S)' centre and the polymer substituent of the resins and monolith. Suzuki–Miyaura and Mizoroki–Heck catalysis exhibit anticipated trends in reactivity with variation of aryl halide reagents for each system, and show that supported catalysis on beads and monolith gives higher yields than for homogeneous catalysis. The synthesis of 2-methylthiomethylpyridines is presented, together with crystal structures of 4-bromo-2-bromomethylpyridine hydrobromide, 4-(4-hydroxyphenyl)-2-methylthiomethylpyridine (L^1), $PdCl_2(L^1)$ and $PdCl_2(L^2)$. Hydrogen bonding occurs in 4-bromo-2-bromomethylpyridine hydrobromide as N–H···Br interactions, in 4-(4-hydroxyphenyl)-2-methylthiomethylpyridine as O–H···N to form chains, and in $PdCl_2(L^1)$ as O–H···Cl interactions leading to adjacent π-stacked chains oriented in an antiparallel fashion.

1. Introduction

We have recently examined the ability of palladium(II) complexes of neutral 2-organothiomethylpyridine-*N*,*S* donor ligands to facilitate Mizoroki–Heck catalysis, in order to explore potential roles for heteroleptic ligands that may exhibit hemilabile activity during the catalytic cycle (Fig. 1).[1] The role of this ligand motif in palladium catalysis has also been explored by Chelucci for addition of diethylzinc to benzaldehyde[2a,b] and for allylic substitution,[2a] and by Canovese for trimerisation of dimethylacetylene dicarboxylate,[2c] and the stoichiometric synthesis of fluoranthenes[2d–f] and 2,4-diene-6-ynes.[2f] We have recently commenced the development of flow-through capillary[3] and chip[3b] based microreactors (100–250 μm internal diameter) employing continuous macroporous organic monolith as support for palladium-catalysed Suzuki–Miyaura[3] and Sonogashira[3c] reactions. This flow-through

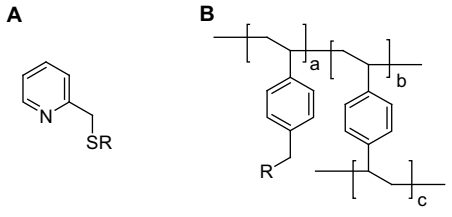

Figure 1. (A) 2-Organothiomethylpyridine ligands (R=Me, Ph). (B) Polymeric supports (i) Merrifield resin [R=Cl, typically 2–3% divinylbenzene (DVB) crosslinker]; (ii) Wang resin [R=*p*-$BrCH_2C_6H_4O$, typically 1% DVB]; and (iii) poly(chloromethylstyrene-*co*-divinylbenzene) monolith (CMS/DVB, R=Cl, typically CMS/DVB ratio ∼3:2 and (CMS/DVB)/(porogen) ratio ∼2:3 in preparations to give highly porous continuous polymeric monolith).

* Corresponding authors. Tel.: +61 3 6226 2162; fax: +61 3 6226 2858.
E-mail addresses: rcj@utas.edu.au (R.C. Jones), allan.canty@utas.edu.au (A.J. Canty).

0040-4020/$ – see front matter © 2009 Elsevier Ltd. All rights reserved.
doi:10.1016/j.tet.2009.07.013

technology to date has mainly utilised 1,10-phenanthroline and *N*-methylimidazole moieties,[3] e.g., attack by 5-amino-1,10-phenanthroline at the benzylic chloride group of poly(chloromethylstyrene-*co*-divinylbenzene) monolith [CMS/DVB, Fig. 1B(iii)], and with *N*-methylimidazole to most likely form palladium(II) carbene species on addition of $PdCl_2(NCMe)_2$.[3c]

The principles of flow-through organic synthesis at the microscale level in capillaries and chips of internal dimensions $<\sim$1 mm have been elucidated recently.[4] Advantages over conventional reaction systems include high surface/volume ratio leading to excellent heat transfer allowing higher concentrations and better selectivity in reactions, environmental and safety advantages from use of less solvent and reagents, synthesis of quantities of product sufficient for biological assay and integration with analysis instrumentation, significant advantages in simplicity of scale-out via multiple microreactors in parallel, together with applications in combinatorial chemistry. For metal catalysis in capillary[5] and chip[6] microreactors (internal diameter $<\sim$1 mm), innovative systems developed to date have included homogeneous catalysis in open tubes/channels,[5c,e,6c] homogeneous with gas/liquid interface,[6e] palladium as nanoparticles,[5b] palladium[5d] or gold[5h] thin film on internal walls, palladium thin film together with complex,[5g] palladium on metal oxide particles[5a,6a,b] and on polysilane/metal oxide particles[5f] and, in our recent reports, palladium complexes supported on continuous organic polymer monolith[3] (e.g., Fig. 1B(iii)).[3b,c] For supported catalysis, the latter approach avoids difficulties in filling capillaries with particles and in confining particles within capillaries, difficulties associated with swelling of polymer beads and compaction of particles if high pressure is required for flow-through operation. The monolith is fully anchored to walls during synthesis, the solid phase is uniform with absence of particles, and the void volume fraction for the monolith used in the present study is 79%. Organic polymer monoliths have high surface area and excellent flow-through properties.[7]

These promising developments are explored further here via the synthesis and characterisation of an *N*,*S*-heteroleptic motif known to be active in several palladium-catalysed processes and organic syntheses functionalised by *p*-HOC_6H_4 at the 4-position allowing covalent attachment to organic polymer supports (Fig. 1A; R=Me). Mizoroki–Heck and Suzuki–Miyaura cross-coupling activity is examined for '$[PdCl_2(N,S)]$' complexes, and compared with supported catalysis where the ligand is attached to Merrifield and Wang beads (Fig. 1B(i) and B(ii)), ground bulk monolith, and the dichloropalladium(II) complex of a closely related ligand as a homogeneous catalyst. To date, *N*,*S*-bidentate ligands do not appear to have been explored in Suzuki–Miyaura catalysis.

2. Results and discussion

2.1. Ligand synthesis

For the ligand motif A (R=Me) (Fig. 1) the pyridine and thiomethyl groups are anticipated to be unreactive towards the benzylic halide group of the organic polymers B. A suitable reagent containing this motif, and facilitating covalent attachment to the polymers, could include a hydroxyl group. To achieve this, functionalisation of the 4-position of the pyridine ring with a phenolic group was considered desirable in order to minimise any steric interaction between the phenolic group and the metal centre. The synthesis in Scheme 1 was developed based on the reaction of commercially available **1** with acetyl bromide to give **2** with slight modification of a reported method[8] (glacial acetic acid as solvent rather than neat reagents) to increase the yield from 31 to 91%; employing the protocol of van den Heuvel et al. (trifluoroacetic anhydride to generate 4-bromo-2-trifluoroacetoxymethylpyridine, followed by hydrolysis with NaOH)[9a] for synthesis of the 5-bromo analogue to obtain known compound[9b] **3** (62%); bromination of **3** to give **4** (87%), a modification of the protocol of Canovese et al. (reaction with thiomethoxide)[10] for the synthesis of related compounds to give **5** (72%); and Suzuki–Miyaura chemistry to give **6** (90%; overall yield 32%). Compound **7** was synthesised as a model for the benzyl ether connectivity between ligand and the polymer backbone (overall yield 30%), and palladium(II) complexes of **6** and **7**, $PdCl_2(L^1)$ (**8**) and $PdCl_2(L^2)$ (**9**), respectively, were obtained on reaction with $PdCl_2(NCMe)_2$ under reaction conditions identical to those used to add palladium(II) to polymers functionalised with compound **6**.

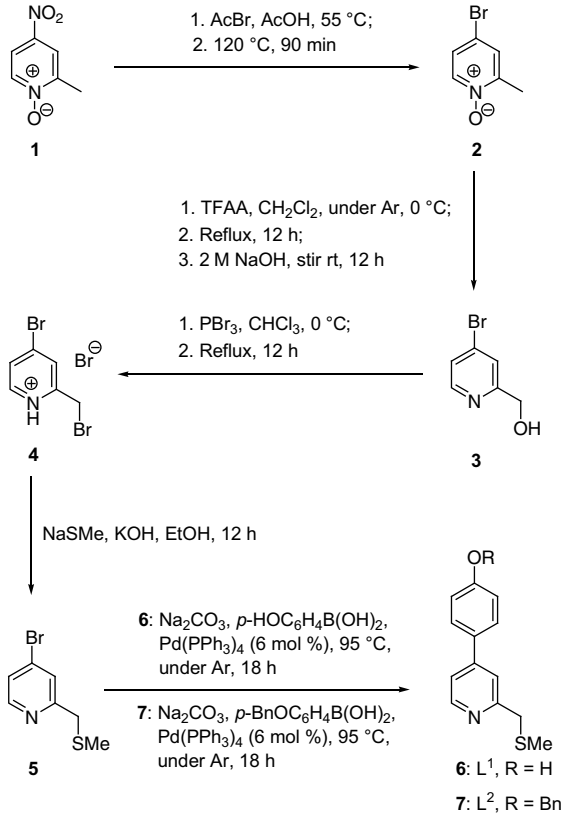

Scheme 1. Synthesis of 2-methylthiomethylpyridines **6** and **7**.

NMR spectra were readily interpreted, noting that **6** alone, containing the phenol group, undergoes deuterium exchange of the methylene group in $(CD_3)_2CO$ providing that D_2O is present, attributed to tautomeric and mesomeric effects encouraging exchange via **IV**, which is illustrated in Scheme 2; X-ray structural data (see below) indicate little if any contribution from the 'pyridone' form **III** in the solid state.

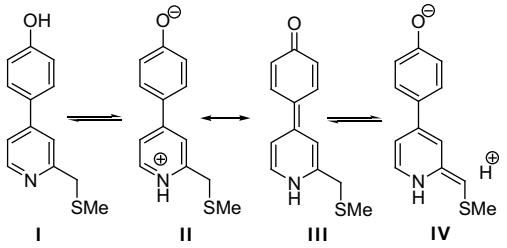

Scheme 2.

2.2. X-ray crystal structures of reagents and palladium(II) complexes as models for the supported catalyst

Aspects of the structure of reagents **4**, **6** and complexes **8**, **9** are illustrated in Figures 2 and 3. The compounds containing a phenolic hydroxy group (as well as the hydrobromide salt **4**) exhibit hydrogen bonding, for which refinement of the hydrogen atom positions indicate N–H···Br^- interaction in **4**, O–H···N in **6** and O–H···Cl in **8**. The N···Br distance in **4**, 3.139(7) Å, is similar to that reported for 2,6-bis(bromomethyl)pyridinium bromide, 3.242(2) Å.[11] Other close bromide contacts are a π-face of a pyridyl ring, a methylene proton, a 6H-pyridyl and Br of a 2-CH_2Br substituent. Molecules of **6** form linear polymeric chains through O–H···N hydrogen bonding involving the pyridyl nitrogen and phenolic substituent. These arrange themselves into parallel running stacks displaying limited π-stacking between adjacent pyridyl and aryl rings owing to disruptions brought about by the positioning of the methylene protons and the torsion angle of aromatic rings in the molecule. The O···N distance (2.700(3) Å) is similar to that reported for 4-(3,5-dimethylpyridin-4-yl)-3,5-dimethylphenol, 2.721(2) Å.[12] Consistent with the presence of C–O–H···N in **6**, rather than C=O···H–N that could be anticipated for tautomer **III**, the C–O and inter-ring C–C distances, 1.353(3) and 1.476(3) Å, respectively, are both much longer than quinoidal structures [~1.222 and ~1.349 Å].[13] The ring–ring dihedral angle, 29.9(2)°, is also supportive of the absence of inter-ring multiple bonding.

Complexes **8** and **9** exhibit distorted square planar coordination geometries (Fig. 3). As for the free ligand **6**, molecules of **8** form hydrogen-bonded linear polymeric chains in the solid state, though these involve OH···Cl interactions involving a chloride ligand (trans to S) and the phenolic substituent. In contrast to **6**, these polymeric strands stack antiparallel into dimeric units involving offset face–face π-stacking that is aided by the near planar aryl–pyridyl moieties allowing an intermolecular distance of 3.43(2) Å. Palladium coordination planes between paired sets of chains are close to being directly aligned, but the Pd···Pd contact of 3.711(3) Å indicates the absence of a metal–metal interaction (van der Waals radius 1.63 Å).[15] The polymeric chain structure is similar to those reported

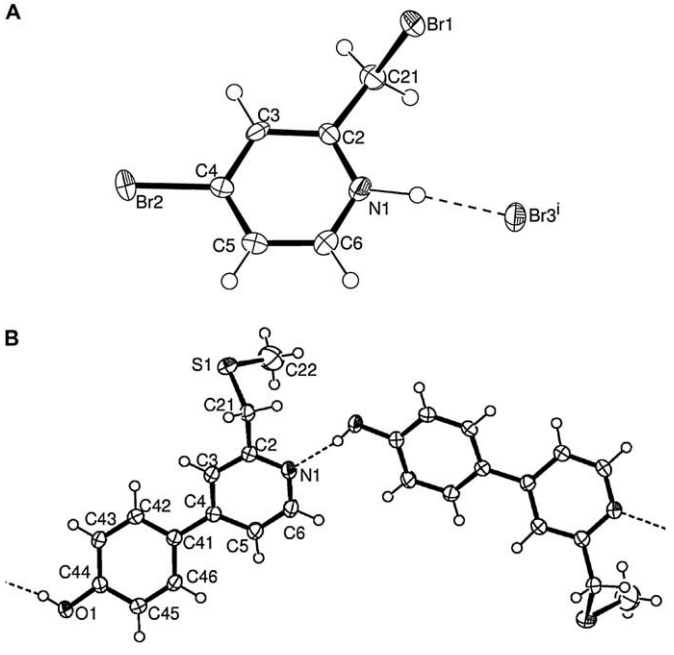

Figure 2. Molecular structures of **4** (A) [symmetry code: (i) $-x-1/2$, $y+1/2$, $-z+1/2$] and **6** (B). For **6**, the partial packing diagram shows a portion of the linear polymeric strands resulting from hydrogen bonding.

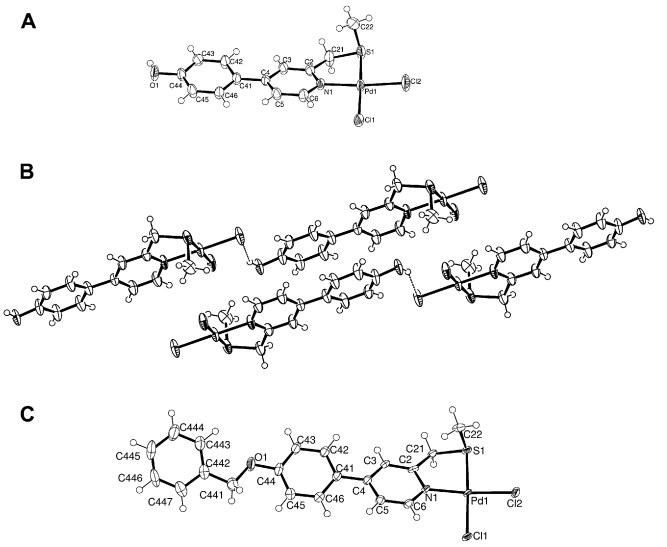

Figure 3. Molecular structures of $PdCl_2(L^1)$ (**8**) (A) and $PdCl_2(L^2)$ (**9**) (C). For **8**, the partial packing diagram (B) shows the antiparallel arrangement of the linear polymeric strands resulting from hydrogen bonding. Palladium–donor atom distances [N1 2.039(8), 2.037(3); S1 2.247(3), 2.2617(9); Cl1 (trans to S1) 2.321(3), 2.3305(9); Cl2 (trans to N1) 2.299(3), 2.2967(10) Å, for **8** and **9**, respectively] and chelate angles [84.5(2)°, 84.58(6)°] are similar to values reported for related Pd(II) complexes.[14] The pyridyl mean plane forms a dihedral angle of 16.2(4)° (**8**) and 18.9(1)° (**9**) with the mean metal coordination plane, the aryl/pyridyl inter-ring dihedral angles are 8.1(7)° (**8**) and 19.8(2)° (**9**), and the C–O and inter-ring C–C distances of both **8** and **9** are within 1 esd of those for ligand **6**.

for '[ECE]' (E=N, S) pincer complexes having a hydroxyl group hydrogen-bonded to a chloro-ligand in $MCl\{C_6H_2(CH_2NMe_2)_2$-2,6-OH-4} (M=Pt,[16a,b] Pd[16c]) and $PdCl\{C_6H_2(CH_2SPh)_2$-2,6-OH-4}[16c], which have O–H···Cl with O···Cl 3.1040(18)–3.127(8) Å compared with 3.002(8) Å in **8**.

For complex **9**, the linear polymeric chains noted for **6** and **8** are absent as hydrogen bonding is absent. Some packing features are retained in that there is rough alignment of the, now, quite extended polyaromatic ligand framework in the overall structure. π-Stacking between molecules is limited to the central aryl rings (3.632 Å) that extends indefinitely. The limited π-stacking, in relation to complex **8**, is presumably due to the influences of the greater torsion angle between the pyridyl and aryl rings (19.8(2)°) and the incorporation of the saturated benzylic carbon centre of the ether substituent. Coplanarity of metal coordination planes (3.633(2) Å) within these stacks is noted, however, the metal centres are offset somewhat, giving a metal–metal separation of 5.133(1) Å.

2.3. Formation of polymer with supported precatalyst sites

As illustrated in Scheme 3, commercially obtained polymer beads were treated with reagent **6** in ethanol at 60 °C in the presence of excess base (*i*-Pr_2NEt or Bu_4NOH). Similar results were obtained for both bases. Scanning electron micrographs of Merrifield beads indicated considerable bead fragmentation after this treatment, as reported for a recent study of catalyst immobilisation,[17] but Wang beads were unaffected. Ground bulk monolith and capillaries filled with continuous monolith, obtained as documented,[3c] were treated with ligand **6** in a similar manner, following the documented protocol,[3c] and for capillaries involved flow-through of the solution in each direction. The base Bu_4NOH was used for ligand attachment to monolith as it promotes higher solubility of **6** than does *i*-Pr_2NEt, and thus minimises the possibility of precipitation. Subsequently, the systems were treated with

$PdCl_2(NCMe)_2$ under identical conditions, matching that for the synthesis of $PdCl_2(L^1)$ (**8**) and $PdCl_2(L^2)$ (**9**). A scanning electron micrograph of bulk monolith after attachment of ligand and palladium (Fig. 4) is unchanged in appearance from that prior to attachment, and appears similar to monolith obtained on attachment of other ligands.[3c] Palladium analysis showed levels of 0.75 wt % (Merrifield resin), 0.32 wt % (Wang) and 1.19 wt % (bulk monolith). Analysis for capillaries was not attempted as essentially identical conditions were used for funtionalisation of the monolith in bulk and in capillaries. The capillaries (internal diameter 250 μm, length 30 cm) were cut to 10 cm lengths for catalytic studies.

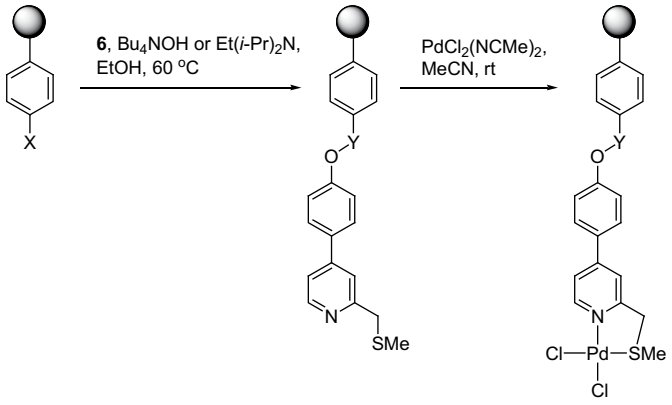

Scheme 3. Functionalisation of Merrifield resin and monolith (X=CH_2Cl, Y=CH_2) or Wang resin (X=$CH_2OC_6H_4CH_2Br$, Y=$CH_2OC_6H_4CH_2$).

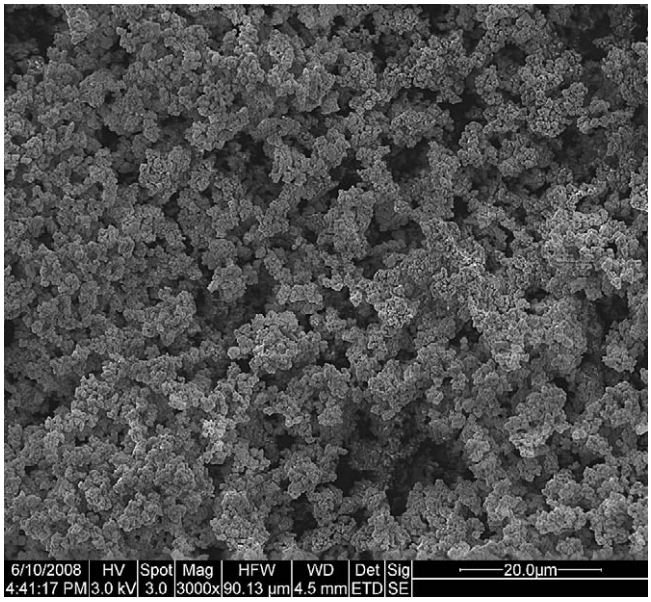

Figure 4. Scanning electron micrograph of ground bulk monolith after attachment of ligand and palladium (×3000, accelerating voltage 3.0 kV).

2.4. Studies of Suzuki–Miyaura and Mizoroki–Heck catalysis

In addition to the supported systems, catalysis using the model complex $PdCl_2(L^2)$ (**9**) was undertaken as the ligand L_2 contains the same benzyl ether linker on its periphery as that present in the ligand motif attached to solid supports. Direct comparison between catalysis for this complex, the resins, bulk monolith and capillary systems is problematic, mainly due to the different experimental protocol required for flow-through studies. Microreactors have a much higher effective mol % precatalyst in the flow-through architecture, as noted previously.[17] Thus, for the 10 cm length capillary of internal diameter 250 μm filled with monolith of mass 1.76 mg and 1.19 wt % Pd, a void volume fraction of 79% results in an effective mol % Pd of ~51% for an aryl halide concentration of 0.1 M.

However, an approximate comparison between beads, bulk monolith and homogeneous catalysis is feasible as the homogeneous catalysis can be conducted using the same mol % precatalyst. To ascertain whether palladium was not simply adhered to the solid phase, support materials that had not been treated in any way, or treated with ligand only, or treated with $PdCl_2(NCMe)_2$ only followed by flushing, did not act as catalysts in Mizoroki–Heck reactions, and for these trials palladium could not be detected in the supports by ICP-MS analysis.

Reactions studied are illustrated in Scheme 4 and results are presented in Tables 1 and 2. For beads, bulk monolith and homogeneous systems the preferred base Na_2CO_3 was used, but for capillaries Et_3N was used as Na_2CO_3 has low solubility that may lead to blockages.

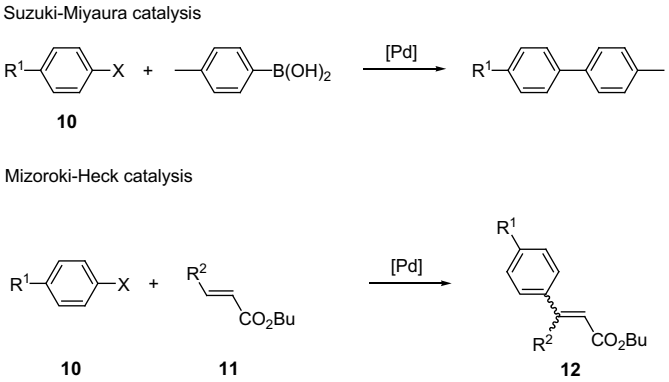

Scheme 4.

For both Suzuki–Miyaura and Mizoroki–Heck reactions using beads and bulk monolith (Table 1), similar results are obtained for each support, with trends on variation of reagent as expected, in particular aryl iodides>bromides>chlorides, e.g., for Suzuki–Miyaura (PhI>PhBr>*p*-AcC_6H_4Cl, entries 1–3); and for Mizoroki–Heck (PhI>PhBr>*p*-TolBr>*p*-AcC_6H_4Cl and PhCl, entries 5–9, and PhI>PhBr, entries 10 and 11). High yields of the trisubstituted Mizoroki–Heck product were obtained (entries 10 and 11). Moderate activation of 4-chloroacetophenone in the Mizoroki–Heck reaction (entry 3) indicates that further development of catalyst design may lead to improved aryl chloride activation. For both catalysis systems, the solid supports provide higher yield than comparable homogeneous catalysis (entries 2, 4 and 6, 12), and the homogeneous systems provide lower yields than widely used phosphine systems.[18]

Detailed comparison of values obtained from different bulk supports is difficult in view of the differing mol % of precatalyst and differences in anticipated access of reagents to precatalyst sites, e.g., observed fracture of the Merrifield beads compared with unaltered appearance of Wang beads, and anticipated better access to interior sites for monolith than for beads. However, for bulk reactions the trend in loadings (monolith>Merrifield>Wang) is reflected in the same trend in yield (entries 3, 5–7, 10). If it is assumed that precatalyst sites have identical activities for the three supported systems, trends in turnover number (TON) may reflect the accessibility of sites. Thus, it is of interest to note that, except where yields are >99% or very low (entry 9, Wang entries 3 and 8), turnover numbers (TON, moles of product/moles of palladium) for Merrifield and Wang beads are greater than those for monolith (entries 3, 6–8, 11), even when the yield is lower for beads (entries 3 and 8). Leaching of palladium could not be detected by ICP-MS analysis above background levels that were obtained in blank runs using reagents and the three supports without precatalyst.

Table 1
Comparison of Suzuki–Miyaura and Mizoroki–Heck catalysis for Merrifield and Wang beads and ground monolith with anchored palladium(II) precatalyst, and homogeneous catalysis using $PdCl_2(L^2)$ (**9**) as precatalyst[a]

Entry	X	**10** (R^1)	**11** (R^2)	Yield (%)			TON
				Merrifield	Wang	Monolith	
Suzuki–Miyaura, beads and monolith							
1	I	H		>99	>99	>99	8512, 19,950, 5365
2	Br	H		>99	85	>99	8512, 16,958, 5365
3	Cl	Ac		8	<1	12	681, <199, 644
Suzuki–Miyaura, homogeneous, identical mol % loading as analogous supported catalysis							
4	Br	H		57	6.4	64	4852, 1227, 3434
Mizoroki–Heck, beads and monolith							
5	I	H	H	>99	>99	>99	8512, 19,950, 5365
6	Br	H	H	95	86	93	8086, 17,157, 4989
7	Br	Me	H	85	70	78	7235, 13,965, 4185
8	Cl	Ac	H	12	<1	15	1021, <199, 804
9	Cl	H	H	<1	<1	1	<85, <199, 54
10	I	H	Ph	>99	>99	>99	8512, 19,950, 5365
11	Br	H	Ph	85	72	87	7235, 14,364, 4668
Mizoroki–Heck, homogeneous, identical mol % loading as analogous supported catalysis							
12	Br	H	H	6	<1	11	511, <199, 590

[a] Reagents shown in Scheme 3. Suzuki–Miyaura conditions: ArX (**10**, 0.3 M), *p*-TolB$(OH)_2$ (0.45 M), polymer (5 mg), Na_2CO_3 (0.6 M) in DMF/H_2O (3:1, 10 mL), 80 °C, 24 h. Mizoroki–Heck conditions: ArX (**10**, 0.3 M), alkene (**11**, 0.45 M), polymer (5 mg), Na_2CO_3 (0.6 M), Bu_4NCl (0.45 M) in DMA (10 mL), 120 °C, 48 h. Merrifield beads and homogeneous catalysis: 0.012 mol % Pd. Wang beads and homogeneous catalysis: 0.005 mol % Pd, monolith and homogeneous catalysis: 0.019 mol % Pd.

Table 2
Suzuki–Miyaura and Mizoroki–Heck catalysis in capillary microreactors[a]

Entry	X	**10** (R^1)	**11** (R^2)	Yield (%)
Suzuki–Miyaura				
1	I	H		96
2	Br	H		65
Mizoroki–Heck				
3	I	H	H	98
4	Br	H	H	45

[a] ~39 min contact time of reagent solution within capillaries of internal diameter 250 μm, length 10 cm, flow rate 0.1 μL min^{-1}; ~51 mol % Pd. Suzuki–Miyaura conditions: ArX (**10**, 0.10 M), *p*-TolB$(OH)_2$ (0.15 M), Et_3N (0.2 M) in DMF/H_2O (3:1), 80 °C, 24 h. Mizoroki–Heck conditions: ArX (**10**, 0.10 M), alkene (**11**, 0.15 M), Et_3N (0.2 M) in DMA, 120 °C, 24 h.

Results for the bulk studies demonstrate that the *N*,*S*-bidentate system facilitates catalysis. The capillary microreactor was examined for reaction of iodo- and bromobenzene, and the same trend in reactivity was observed for both catalyses (entries 1, 2 and 3, 4) (Table 2), illustrating the feasibility of this microreactor technology. Assuming that the palladium loading is identical to that of the bulk monolith, leaching of Pd over a 24 h period corresponded to ~0.05% for the Suzuki–Miyaura and Mizoroki–Heck reactions.

3. Experimental section

3.1. General techniques

All solvents were dried and distilled by conventional methods prior to use. 4-Nitro-2-picoline *N*-oxide (Oakwood), 4-hydroxyphenylboronic acid (Boron Molecular), (chloromethyl)polystyrene (Merrifield Resin, 200–400 mesh, 37–74 μm) (Fluka), (4-bromomethylphenoxymethyl)polystyrene (Wang Resin, 100–200 mesh, 74–149 μm) (Novabiochem), ultra high purity argon (BOC Gases) and other reagents (Aldrich) were used as received. Bulk monolith and fused silica capillaries (internal diameter 250 μm, outer surface coated with polyimide (Polymicro Technologies, Phoenix, Arizona)) filled with monolith bonded to the walls were prepared as reported.[3c] Bulk monolith was ground, resulting in a range of particle sizes up to ~200 μm. NMR spectra were recorded at 20 °C on a Varian Mercury Plus 300 spectrometer and chemical shifts are reported in parts per million relative to TMS; assignments were facilitated by gHMBC, gHMQC and gCOSY techniques. For **6** and **8** the C_6H_4 group atoms are denoted H4b and H4c; for **7** and **9** the phenyl group atoms are denoted H4b–d2. Microanalyses, LSIMS mass spectra, scanning electron micrographs (FEI Quanta 600 MLA ESEM) and ICP-MS (ELEMENT high resolution) allowing detection down to 0.1 ppb were performed by the Central Science Laboratory. GC–MS measurements were performed using a Varian 3800 gas chromatograph coupled with a triple quadrupole mass spectrometer; GC-FID measurements were performed on a Shimadzu GC-2014 AFsc gas chromatograph equipped with a 25 m length (ID 0.32 mm) ID-BPX5 SGE capillary column. Standards were purchased or synthesised using conventional techniques, and mixtures with different concentration ratios were used for calibration. The mass of monolith in a capillary was determined using a Sartorius SE2 Ultra-Microbalance (0.1 μg readability), and the void volume fraction was determined as described previously.[3c] For palladium analyses, samples (50–100 mg) were digested in freshly prepared *aqua regia* (4 mL) for 18 h with sonication, diluted to a final mass of 30 g, indium (100 ppb) was added as an internal standard, and measurements performed on the low resolution setting of $300m\ (\Delta m)^{-1}$ at 10% valley definition, and palladium was measured as a total of isotopes 105, 106 and 108.

For microreactor catalysis, as reported,[3c] controlled solvent pumping was performed using a Harvard Apparatus model PHD 2000 (Holliston, Massachusetts, USA) twin syringe pump and 250 μL Hamilton (Reno, Nevada, USA) Gastight® glass syringes. All capillaries and syringes were connected using Upchurch Scientific

(Oak Harbor, Washington, USA) capillary connections. Capillaries were heated using a Waters Millipore (Billerica, Massachusetts, USA) 112/WTC-120 temperature controlled column heater. Leading and trailing capillary sections were used to ensure that the whole microreactor was inside the column heater.

3.2. Synthetic procedures

*3.2.1. 4-Bromo-2-methylpyridine N-oxide (**2**)*

Acetyl bromide (34.6 mL, 0.46 mol) was added in small portions to a solution of 4-nitro-2-picoline *N*-oxide (2.47 g, 0.02 mol) in glacial AcOH (35 mL) at 55 °C. The resulting solution was heated to 120 °C with stirring for 2.5 h in air. After cooling to rt the solution was poured into crushed ice and made basic with K_2CO_3 and the product extracted with CH_2Cl_2 (4×30 mL). The combined organic phases were washed with brine, and dried over Na_2SO_4. The solvent was removed in vacuum resulting in a pale orange oil, which was used without further purification (2.75 g, 91%). ^{1}H NMR (300 MHz, $CDCl_3$): δ 8.11 (d, J=6.9 Hz, 1H, H6), 7.41 (d, J=2.4 Hz, 1H, H3), 7.27 (dd, J=6.9, 2.4 Hz, 1H, H5), 2.48 (s, 3H, CH_3); ^{13}C{^{1}H} NMR (75.4 MHz, $CDCl_3$): δ 150.6 (C2), 140.2 (C6), 129.6 (C3), 127.0 (C5), 119.4 (C4), 17.9 (CH_3). MS (EI) m/z 187 [M$^+$], [$^{12}C_6H_6{}^{79}Br^{14}N^{16}O$ 187]. HRMS (EI) m/z [M−H]$^+$ 186.96339, [C_6H_6BrNO]$^+$ requires 186.96328.

*3.2.2. 4-Bromo-2-hydroxymethylpyridine (**3**)*

Under argon, TFAA (9.24 mL, 66.48 mmol) was added dropwise (with extreme caution) to a solution of **2** (2.50 g, 13.30 mmol) in dry CH_2Cl_2 (40 mL) at 0 °C, and the resulting solution refluxed for 12 h with stirring. After cooling to rt the TFAA and CH_2Cl_2 were removed in vacuum to give a dark yellow oil; CH_2Cl_2 (40 mL) was added followed by 2 M NaOH with vigorous stirring until the resulting biphasic mixture was basic (pH 12–14). Vigorous stirring was continued for 12 h under Ar, and the mixture extracted with CH_2Cl_2 (3×30 mL). The organic phase was washed with brine and dried over Na_2SO_4. The solvent was removed in vacuum resulting in a dark brown oil, which was used without further purification. (1.55 g, 62%). ^{1}H NMR (300 MHz, $CDCl_3$): δ 8.36 (d, J=5.4 Hz, 1H, H6), 7.52 (dd, J=1.8 Hz, 1H, H3), 7.39 (dd, J=5.4, 1.8 Hz, 1H, H5), 4.75 (s, 2H, CH_2), 4.16 (s, 1H, OH); ^{13}C{^{1}H} NMR (75.4 MHz, $CDCl_3$): δ 161.1 (C2), 149.2 (C6), 134.1 (C4), 126.0 (C5), 124.3 (C3), 63.9 (CH_2). MS (EI) m/z 187 [M−H]$^+$, [$^{12}C_6H_5{}^{79}Br^{14}N^{16}O$ 186]. HRMS (EI) m/z [M−H$^+$] 185.95554, [C_6H_5BrNO]$^+$ requires 185.95545.

*3.2.3. 4-Bromo-2-bromomethylpyridine hydrobromide (**4**)*

PBr_3 (5.55 mL, 59.03 mmol) was added dropwise (with extreme caution) to a solution of **3** (1.85 g, 9.84 mmol) in dry $CHCl_3$ (50 mL) at 0 °C, and the resulting solution was heated to reflux for 12 h with vigorous stirring. After cooling to rt the suspension was poured into crushed ice and made basic (pH ~ 14) with K_2CO_3, and the product was extracted with CH_2Cl_2 (4×50 mL). The organic phase was washed with brine and dried over Na_2SO_4. The solvent was removed in vacuum, and the resulting pale brown oil was then dissolved in Et_2O and with vigorous stirring; HBr/AcOH solution was added dropwise to precipitate an off white solid, which was collected by filtration and washed thoroughly with Et_2O (2.84 g, 87%). Single crystals for X-ray and elemental analysis were grown from vapour diffusion of Et_2O into $MeNO_2$. ^{1}H NMR (300 MHz, CD_3OD): δ 8.70 (d, J=6.3 Hz, 1H, H6), 8.42 (d, J=2.1 Hz, 1H, H3), 8.21 (dd, J=6.3, 2.1 Hz, 1H, H5), 4.81 (s, 2H, CH_2); ^{13}C{^{1}H} NMR (75.4 MHz, CD_3OD): δ 153.4 (C2), 144.1 (C4), 143.7 (C6), 130.9 (C5), 130.1 (C3), 24.8 (CH_2). MS (EI) m/z 251 [M−HBr]$^+$, [$^{12}C_6H_5{}^{79}Br_2{}^{14}N$ 251]. HRMS (EI) m/z [M−HBr]$^+$ 248.87875, [$C_6H_5Br_2N$]$^+$ requires 248.87887. Anal. Calcd for $C_6H_6Br_2N$: C, 21.72; H, 1.82; N, 4.22. Found: C, 22.12; H, 1.78; N, 4.20.

*3.2.4. 4-Bromo-2-methylthiomethylpyridine (**5**)*

A stirred solution of NaOMe (0.35 g, 4.97 mmol) in dry EtOH (50 mL) was added dropwise over 10 min to a stirred solution of **4** (1.50 g, 4.52 mmol) and powdered KOH (0.76 g, 13.56 mmol) in dry EtOH (100 mL). Stirring was continued for 12 h after which the EtOH was removed in vacuum resulting in a pale brown oil. Water (25 mL) was added and the product extracted with CH_2Cl_2 (3×25 mL). The organic phase was washed with brine and dried over Na_2SO_4. The solvent was removed in vacuum to give a pale brown oil, which was purified by column chromatography [40% EtOAc in hexanes], to give a pale yellow oil (0.75 g, 72%). ^{1}H NMR (300 MHz, $CDCl_3$): δ 8.34 (d, J=5.4 Hz, 1H, H6), 7.56 (d, J=1.8 Hz, 1H, H3), 7.34 (dd, J=5.4, 1.8 Hz, 1H, H5), 3.76 (s, 2H, CH_2), 2.06 (s, 3H, SCH_3); ^{13}C{^{1}H} NMR (75.4 MHz, CD_3OD): δ 159.1 (C2), 148.6 (C6), 132.7 (C4), 125.4 (C3), 124.4 (C5), 38.5 (CH_2), 14.2 (SCH_3). MS (EI) m/z 218 [M]$^+$, [$^{12}C_7H_8{}^{79}Br^{14}N^{32}S$ 218]. HRMS (EI) m/z [M$^+$] 216.95611, [C_7H_8BrNS]$^+$ requires 216.95608.

*3.2.5. 4-(4-Hydroxyphenyl)-2-methylthiomethylpyridine (**6**)*

$Pd(PPh_3)_4$ (0.397 g, 5 mol %) and **5** (1.50 g, 6.88 mmol) in toluene (28.0 mL) were treated with a degassed solution of Na_2CO_3 (1.60 g, 13.11 mmol, 2.2 equiv) in H_2O (14.0 mL), followed by a solution of p-$HOC_6H_4B(OH)_2$ (1.42 g, 10.32 mmol) in MeOH (10.0 mL). The resulting mixture was stirred at 95 °C under Ar; after 6 h another 0.5 equiv of p-$HOC_6H_4B(OH)_2$ and a further 1 mol % of catalyst was added to the solution, and after 12 h the solution was cooled to rt and treated with a saturated solution of Na_2CO_3. The product was extracted with CH_2Cl_2 (3×25 mL), the organic phase was washed with saturated NaCl solution, dried over Na_2SO_4 and the solvent removed in vacuum to give a dark oil. The oil was dissolved in CH_2Cl_2 (5 mL) and hexane added to precipitate a tan solid (1.56 g, 98%). The product was recrystallised from hot EtOH to give a dark brown solid (1.43 g, 90%). ^{1}H NMR (300 MHz, $(CD_3)_2CO$): δ 9.01 (s, 1H, OH), 8.47 (dd, J=5.1, 1.5 Hz, 1H, H6), 7.66 (m, 3H, H3, H4b), 7.47 (dd, J=5.1, 1.5 Hz, 1H, H5), 6.83 (d, J=8.7 Hz, 2H, H4c), 3.82 (s, 2H, CH_2), 2.08 (s, 3H, SCH_3); ^{13}C{^{1}H} NMR (75.4 MHz, $(CD_3)_2CO$): δ 159.7 (C2), 158.1 (*C*OH), 149.8 (C6), 149.7 (C4), 128.7 (C4a), 128.4 (C4b), 119.8 (C3), 119.0 (C5), 116.3 (C4c), 39.8 (CH_2), 14.5 (SCH_3). MS (APCI) m/z 232 [M+H]$^+$, [$^{12}C_{13}H_{14}{}^{14}N^{16}O^{32}S$ 232]. HRMS (EI) m/z [M+H]$^+$ 232.07941, [$C_{13}H_{14}NOS$]$^+$ requires 232.07961. Anal. Calcd for $C_{13}H_{13}NSO$: C, 67.50; H, 5.66; N, 6.06. Found: C, 67.54; H, 5.62; N, 6.11.

*3.2.6. 4-(4-Benzyloxy)-2-methylthiomethylpyridine (**7**)*

This compound was prepared from **5** (1.50 g, 6.88 mmol) and 4-$BnOC_6H_4B(OH)_2$ (2.35 g, 10.32 mmol) using a similar procedure to that described for **6**. The product was purified by column chromatography (40% EtOAc in hexanes) to remove contamination by BnOPh to give a pale yellow oil (1.88 g, 85%). ^{1}H NMR (300 MHz, $(CD_3)_2SO$): δ 8.53 (d, J=5.4 Hz, 1H, H6), 7.76 (dd, J=5.4, 1.8 Hz, 1H, H5), 7.60 (d, J=8.7 Hz, 2H, H4b), 7.56 (d, J=1.8 Hz, 1H, H3), 7.46–7.34 (m, 5H, H4b2, H4c2, H4d2), 7.07 (d, J=8.7 Hz, 1H, H4c), 5.12 (s, 2H, OCH_2), 3.86 (s, 2H, SCH_2), 2.10 (s, 3H, SCH_3); ^{13}C{^{1}H} NMR (75.4 MHz, $(CD_3)_2SO$): δ 160.1 (C2), 158.9 (C4d), 149.4 (C6), 149.1 (C4), 136.8 (C4a2), 128.9 (C4b), 128.6 (C4c2), 128.4 (C4d2), 127.7 (C4b2), 120.7 (C5), 119.8 (C3), 115.7 (C4c), 70.0 (OCH_2), 40.0 (SCH_2), 22.9 (SCH_3). MS (EI) m/z 321 [M]$^+$, [$^{12}C_{20}H_{19}{}^{14}N^{16}O^{32}S$ 321]. HRMS (EI) m/z [M$^+$] 321.11868, [$C_{20}H_{19}NOS$]$^+$ requires 321.11873. Anal. Calcd for $C_{13}H_{13}NSO$: C, 67.50; H, 5.66; N, 6.06. Found: C, 67.54; H, 5.62; N, 6.11.

*3.2.7. Dichloro{4-(4-hydroxyphenyl)-2-methylthiomethylpyridine}palladium(II) (**8**)*

$PdCl_2(NCMe)_2$ (0.15 g, 0.64 mmol) was added to a stirred suspension of **6** (0.18 g, 0.77 mmol) in dry MeCN (30 mL) and the brown suspension was stirred for 12 h at 50 °C. The solvent was

then reduced in vacuum to ~5 mL and Et_2O was added to precipitate the title complex as a yellow solid, which was collected by filtration and washed with Et_2O (0.23 g, 87%). Single crystals suitable for X-ray structure determination and elemental analysis were grown from a vapour diffusion of Et_2O into $MeNO_2$. ^1H NMR (300 MHz, $(CD_3)_2SO$): δ 10.18 (s, 1H, O*H*), 8.99 (dd, *J*=6.6, 1.8 Hz, 1H, H6), 8.04 (d, *J*=1.8 Hz, 1H, H3), 7.83 (dd, *J*=6.6, 1.8 Hz, 2H, H5), 7.78 (d, *J*=9.0 Hz, 2H, H4b), 6.91 (d, *J*=8.7 Hz, 2H, H4c), 4.76, 4.47 (AB spin system, *J*=16.5 Hz, 2H, C*H*$_2$), 2.55 (s, 3H, SC*H*$_3$); $^{13}C\{^1H\}$ NMR (75.4 MHz, $(CD_3)_2SO$): δ 163.8 (C2), 160.9 (HO*C*), 151.7 (C6), 150.5 (C4), 129.7 (C4b), 125.7 (C4a), 120.7 (C5), 120.4 (C3), 117.0 (C4c), 45.3 (*C*H$_2$), 22.9 (S*C*H$_3$). MS (LSIMS) *m*/*z* 373 $[M-Cl]^+$, $[^{12}C_{13}H_{13}{}^{35}Cl^{14}N^{32}S^{16}O$ 373]. HRMS (EI) *m*/*z* $[M-Cl]^+$ 371.94412, $[C_{13}H_{13}ClNSO]^+$ requires 371.94521. Anal. Calcd for $PdC_{13}H_{13}NSOCl_2$: C, 38.21; H, 3.21; N, 3.43; S, 7.85. Found: C, 38.30; H, 3.07; N, 3.67; S, 7.45.

*3.2.8. Dichloro{4-(4-Benzyloxy)-2-methylthiomethylpyridine}palladium(II) (**9**)*

$PdCl_2(NCMe)_2$ (0.15 g, 0.64 mmol) was added to a stirred suspension of **7** (0.25 g, 0.77 mmol, 1.2 equiv) in dry MeCN (30 mL), instantly affording a bright yellow suspension, which was stirred for 12 h at rt. The solvent was reduced in vacuum to ~5 mL and Et_2O was added. The title complex was collected by filtration as a bright yellow solid and washed with Et_2O (0.27 g, 85%). Single crystals suitable for elemental analysis were grown from hot $MeNO_2$. ^1H NMR (300 MHz, $(CD_3)_2SO$): δ 9.02 (dd, *J*=6.3, 1.8 Hz, 1H, H6), 8.10 (d, *J*=1.8 Hz, 1H, H3), 7.89 (m, 3H, H5, H4b), 7.39 (m, 5H, H4b2, H4c2, H4d2), 7.19 (d, *J*=8.7 Hz, 1H, H4c), 5.19 (s, 2H, OC*H*$_2$), 4.77, 4.48 (AB spin system, *J*=16.8 Hz, 2H, SC*H*$_2$), 2.55 (s, 3H, SC*H*$_3$); $^{13}C\{^1H\}$ NMR (75.4 MHz, $(CD_3)_2SO$): δ 163.9 (C2), 161.3 (C4d), 151.7 (C6), 150.2 (C4), 137.3 (C4a2), 129.6 (C4b), 129.2 (C4c2), 128.7 (C4d2), 128.5 (C4b2), 127.6 (C4a), 121.1 (C5), 120.9 (C3), 116.4 (C4c), 70.1 (OCH$_2$), 45.3 (SCH$_2$), 22.9 (SCH$_3$). MS (LSIMS) *m*/*z* 463 $[M-Cl]^+$, $[^{12}C_{20}H_{19}{}^{35}Cl^{14}N^{32}S^{16}O$ 463]. HRMS *m*/*z* $[M-Cl]^+$ 461.99107, $[C_{20}H_{19}ClNSO]^+$ requires 461.99215. Anal. Calcd for $PdC_{20}H_{19}NSOCl_2$: C, 48.16; H, 3.84; N, 2.81. Found: C, 47.89; H, 3.74; N, 2.72.

3.3. Structural determinations

Data for **4**, **6** and **8** were collected at −80 °C with an Enraf Nonius TurboCAD4 with Mo Kα radiation (0.71073 Å) on crystals of **4**, **6** and **8** mounted on glass fibres. Data for **9** were collected at −173 °C for crystals mounted on a Hampton Scientific cryoloop at the PX1 beamline of the Australian Synchrotron. Views of the structures are shown in Figures 2 and 3. The structures were solved by direct methods with SHELXS-97, refined using full-matrix least-squares routines against F^2 with SHELXL-97,[19] and visualised using X-SEED.[20] All non-hydrogen atoms were refined anisotropically. Nitrogen-bound and O-bound hydrogen atoms were positionally refined and other hydrogen atoms were placed in calculated positions and refined using a riding model with fixed C–H distances of 0.95 Å (sp^2C–H), 0.99 Å (CH_2), 0.98 Å (CH_3). The thermal parameters of all hydrogen atoms were estimated as $U_{iso}(H)=1.2\,U_{eq}(C)$ except for CH_3 where $U_{iso}(H)=1.5\,U_{eq}(C)$.

3.4. Attachment of ligand and palladium to resins and bulk monolith

A suspension of polymer (0.05 g), **6** (0.08 g) and Bu_4NOH (1.75 mmol) in EtOH (5 mL) was stirred at 60 °C for 24 h, after which the resin was filtered under vacuum, resuspended in EtOH and stirred for 30 min, and recovered again by filtration. The polymer was washed twice more with EtOH and dried in vacuum. The modified polymer and $PdCl_2(NCMe)_2$ (0.70 g) in MeCN (5 mL) were stirred for 24 h at rt, filtered under vacuum, resuspended in MeCN, stirred for 30 min and recovered again by filtration. The polymer was washed twice more with EtOH and dried in vacuum.

3.5. Suzuki–Miyaura catalysis for resins and bulk monolith

Aryl halide (3.0 mmol) was added to a solution of *p*-Tol-B(OH)$_2$ (0.612 g, 4.5 mmol), Na_2CO_3 (0.5 g, 6.0 mmol), catalyst (5.0 mg) in a 3:1 DMF/H_2O mixture (10 mL) under Ar. The resulting mixture was stirred at 80 °C for 24 h under Ar. Once cooled to rt, Ph_2O (0.17 g, 1.0 mmol) was added and an aliquot (1.50 mL) was taken and diluted with CH_2Cl_2, washed three times with a saturated NaCl solution. The organic layer was extracted, dried over $MgSO_4$ and filtered, and analysed by GC-FID and GC–MS.

3.6. Mizoroki–Heck catalysis for resins and bulk monolith

Aryl halide (3.0 mmol) was added to a solution of *n*-butylacrylate (0.75 mL, 4.5 mmol) (or *n*-butylcinnamate for entries 10 and 11 in Table 1), Na_2CO_3 (0.5 g, 6.0 mmol), catalyst (5.0 mg) and *n*-Bu_4NCl (1.25 g, 4.5 mmol) in DMA (10 mL) under Ar. The resulting mixture was stirred at 120 °C for 48 h under Ar. The cooled mixture was treated and analysed as for Suzuki–Miyaura catalysis by GC-FID and GC–MS.

3.7. Ligand and palladium attachment to monolith in capillaries

The monolith filled capillary was flushed with EtOH for 30 min at 60 °C (2.0 μL min^{-1}). A filtered solution of **6** (85 mg) and Bu_4NOH (1.5 mL) in EtOH (3.5 mL) was pumped through the capillary at 60 °C for 18 h (0.2 μL min^{-1}), then the capillary was reversed and the solution was pumped through for a further 8 h (0.5 μL min^{-1}). The capillary was washed with EtOH for 1 h at rt (2.0 μL min^{-1}) to remove unreacted ligand and base. The monolith filled capillary was flushed with MeCN for 30 min at rt (2.0 μL min^{-1}), prior to a filtered solution of $PdCl_2(NCMe)_2$ (10 mg) in MeCN (2 mL) being pumped through the capillary at rt for 8 h (0.5 μL min^{-1}), then the capillary was reversed and the solution was pumped through for a further 18 h (0.2 μL min^{-1}). The capillary was flushed with MeCN for 1 h (2.0 μL min^{-1}).

3.8. Suzuki–Miyaura catalysis for capillaries

To equilibrate the microreactor prior to the reaction, the capillary (10 cm) was flushed with DMF/H_2O (3:1) for 1 h at rt (2.0 μL min^{-1}), then with solvent mixture containing 2 M of Et_3N for 2 h at 80 °C (2.0 μL min^{-1}) with the microreactor placed in the pre-heated column heater. The reaction mixtures were passed through the capillary at a flow rate of 0.1 μL min^{-1} for 24 h. The product was collected from the opposing end and analysed by GC-FID.

3.9. Mizoroki–Heck Catalysis for capillaries

A similar procedure was followed, using DMA initially, then DMA with Et_3N, and reactions were carried out at 120 °C for 248 h.

4. Supplementary data

Crystallographic data for **4**, **6**, **8** and **9** have been deposited with the Cambridge Crystallographic Data Centre with deposition

numbers CCDC 726966–726969; data can be obtained free of charge via www.ccdc.cam.ac.uk/data_request/cif.

Acknowledgements

The present research was supported by the Australian Research Council, Dr. R.M.G. is the recipient of an ARC APD fellowship; Dr. A. Townsend (CSL) and Julian Adams (Australian Synchrotron) are acknowledged for technical support. Data for the structure of **9** were obtained on the PX1 beamline at the Australian Synchrotron, Victoria, Australia. The views expressed herein are those of the authors and are not necessarily those of the owner or operator of the Australian Synchrotron.

References and notes

1. Jones, R. C.; Madden, R. L.; Skelton, B. W.; Tolhurst, V.-A.; White, A. H.; Williams, A. M.; Wilson, A. J.; Yates, B. F. *Eur. J. Inorg. Chem.* **2005**, 1048.
2. (a) Chelucci, G.; Berta, D.; Saba, A. *Tetrahedron* **1997**, *53*, 3843; (b) Chelucci, G.; Berta, D.; Fabbri, D.; Pinna, G. A.; Saba, A.; Ulgheri, F. *Tetrahedron: Asymmetry* **1998**, *9*, 1933; (c) Canovese, L.; Visentin, F.; Chessa, G.; Santo, C.; Levi, C.; Uguagliati, P. *Inorg. Chem. Commun.* **2006**, *9*, 388; (d) Canovese, L.; Visentin, F.; Chessa, G.; Uguagliati, P.; Santo, C.; Maini, L. *J. Organomet. Chem.* **2007**, *692*, 2342; (e) Canovese, L.; Visentin, F.; Santo, C. *J. Organomet. Chem.* **2007**, *692*, 4187; (f) Canovese, L.; Visentin, F.; Levi, C.; Santo, C. *J. Organomet. Chem.* **2008**, *693*, 3324.
3. (a) Bolton, K. F.; Canty, A. J.; Deverell, J. A.; Guijt, R. M.; Hilder, E. F.; Rodemann, T.; Smith, J. A. *Tetrahedron Lett.* **2006**, *47*, 9321; (b) Canty, A. J.; Deverell, J. A.; Gömann, A.; Guijt, R. M.; Rodemann, T.; Smith, J. A. *Aust. J. Chem.* **2008**, *61*, 630; (c) Gömann, A.; Deverell, J. A.; Munting, K. F.; Jones, R. G.; Rodemann, T.; Canty, A. J.; Smith, J. A.; Guijt, R. G. *Tetrahedron* **2009**, *65*, 1450.
4. (a) Fletcher, P. D. I.; Haswell, S. J.; Pombo-Vilar, E.; Warrington, B. H.; Watts, P.; Wong, Y. F.; Zhang, X. *Tetrahedron* **2002**, *58*, 4735; (b) Haswell, S. J.; Watts, P. *Green Chem.* **2003**, *5*, 5240; (c) Watts, P.; Haswell, S. J. *Curr. Opin. Chem. Biol.* **2003**, *7*, 380; (d) Watts, P.; Haswell, S. J. *Chem. Soc. Rev.* **2005**, *34*, 235; (e) Hessel, V.; Löwe, H. *Chem. Eng. Technol.* **2005**, *28*, 267; (f) Brivio, M.; Verboom, W.; Reinhoudt, D. N. *Lab Chip* **2006**, *6*, 329; (g) Kobayashi, J.; Mori, Y.; Kobayashi, S. *Chem. Asian J.* **2006**, 22; (h) Watts, P.; Wiles, C. *Chem. Commun.* **2007**, 443; (i) Haeberle, S.; Zengerle, R. *Lab Chip* **2007**, *7*, 1094; (j) Ahmed-Omer, B.; Brandt, J. C.; Wirth, T. *Org. Biomol. Chem.* **2007**, *5*, 733; (k) Mason, B. P.; Price, K. E.; Steinbacher, J. L.; Bogdan, A. R.; McQuade, D. T. *Chem. Rev.* **2007**, *107*, 2300; (l) Kockmann, N.; Gottsponer, M.; Zimmermann, B.; Roberge, D. M. *Chem.—Eur. J.* **2008**, *14*, 7470.
5. (a) He, P.; Haswell, S. J.; Fletcher, P. D. I. *Appl. Catal., A: Gen.* **2004**, *274*, 111; (b) Basheer, C.; Hussain, F. S. J.; Lee, H. K.; Valiyaveettil, S. *Tetrahedron Lett.* **2004**, *45*, 7297; (c) Comer, E.; Organ, M. G. *Chem.—Eur. J.* **2005**, *11*, 7223; (d) Shore, G.; Morin, S.; Organ, M. G. *Angew. Chem., Int. Ed.* **2006**, *45*, 2761; (e) Shi, G.; Hong, F.; Liang, Q.; Fang, H.; Nelson, S.; Weber, S. G. *Anal. Chem.* **2006**, *78*, 1972; (f) Ueno, M.; Suzuki, T.; Naito, T.; Oyamada, H.; Kobayashi, S. *Chem. Commun.* **2008**, 1647; (g) Shore, G.; Morin, S.; Mallik, D.; Organ, M. G. *Chem.—Eur. J.* **2008**, *14*, 1351; (h) Shore, G.; Organ, M. G. *Chem.—Eur. J.* **2008**, *14*, 9641.
6. (a) Greenway, G. M.; Haswell, S. J.; Morgan, D. O.; Skelton, B. V.; Styring, P. *Sens. Actuators, B: Chem.* **2000**, *63*, 153; (b) He, P.; Haswell, S. J.; Fletcher, P. D. I. *Lab Chip* **2004**, *4*, 38; (c) Jönsson, C.; Lundgren, S.; Haswell, S. J.; Moberg, C. *Tetrahedron* **2004**, *60*, 10515; (d) Kobayashi, J.; Mori, Y.; Kobayashi, S. *Chem. Commun.* **2005**, 2567; (e) Miller, P. W.; Long, N. J.; de Mello, A. J.; Vilar, R.; Passchier, J.; Gee, A. *Chem. Commun.* **2006**, 546.
7. Svec, F.; Huber, C. G. *Anal. Chem.* **2006**, *78*, 2101.
8. Klunder, J. M.; Hoermann, M.; Cywin, C. L.; David, E.; Brickwood, J. R.; Scwartz, R.; Barringer, K. J.; Pauletti, D.; Shih, C.-K.; Erickson, D. A.; Sorge, C. L.; Joseph, D. P.; Hattox, S. E.; Adams, J.; Grob, P. M. *J. Med. Chem.* **1998**, *41*, 2960.
9. (a) van den Heuvel, M.; van den Berg, T. A.; Kellogg, R. M.; Choma, C. T.; Feringa, B. L. *J. Org. Chem.* **2004**, *69*, 250; (b) Ashimori, A.; Ono, T.; Uchida, T.; Ohtaki, Y.; Fukaya, C.; Watanabe, M.; Yokoyama, K. *Chem. Pharm. Bull.* **1990**, *38*, 2446.
10. Canovese, L.; Visentin, F.; Uguagliati, P.; Chessa, G.; Pesce, A. *J. Organomet. Chem.* **1998**, *566*, 61.
11. Lozano, V.; Jones, P. G. *Acta Crystallogr.* **2004**, *C60*, o653.
12. Kang, H.; Facchetti, A.; Jiang, H.; Cariati, E.; Righetto, S.; Ugo, R.; Zuccaccia, C.; Macchioni, A.; Stern, C. L.; Liu, Z.; Ho, S.-T.; Brown, E. C.; Ratner, M. A.; Marks, T. J. *J. Am. Chem. Soc.* **2007**, *129*, 3267.
13. Database of average bond-lengths in organic compounds: Allen, F. H.; Kennard, O.; Watson, D. G.; Brammer, L.; Orpen, A. G.; Taylor, R. *J. Chem. Soc., Perkin Trans. 2* **1987**, S1.
14. (a) Canovese, L.; Visentin, F.; Chessa, G.; Uguagliati, P.; Bandoli, G. *Organometallics* **2000**, *19*, 1461; (b) Canovese, L.; Visentin, F.; Chessa, G.; Uguagliati, P.; Santo, C.; Dolmella, A. *Organometallics* **2005**, *24*, 3297; (c) Canovese, L.; Visentin, F.; Santo, C.; Levi, C.; Dolmella, A. *Organometallics* **2006**, *26*, 5590.
15. Bondi, A. *J. Phys. Chem.* **1964**, *68*, 441.
16. (a) Davies, P. J.; Veldman, N.; Grove, D. M.; Spek, A. L.; Lutz, B. T. G.; van Koten, G. *Angew. Chem., Int. Ed* **1996**, *35*, 1959; (b) Albrecht, M.; Lutz, M.; Schreurs, A. M. M.; Lutz, E. T. H.; Spek, A. L.; van Koten, G. *J. Chem. Soc., Dalton Trans.* **2000**, 3797; (c) Mehendale, N. C.; Lutz, M.; Spek, A. L.; Klein Gebbink, R. J. M.; van Koten, G. *J. Organomet. Chem.* **2008**, *693*, 2791.
17. Phan, N. T. S.; Brown, D. H.; Styring, P. *Green Chem.* **2004**, *6*, 526.
18. (a) Kotha, S.; Lahiri, K.; Kashinath, D. *Tetrahedron* **2002**, *58*, 9633; (b) Whitcombe, N. J.; Hii, K. K.; Gibson, S. E. *Tetrahedron* **2001**, *57*, 7449.
19. Sheldrick, G. M. *SHELX97, Programs for Crystal Structure Analysis*; Universität Göttingen: Germany, 1998.
20. Barbour, L. J. *J. Supramol. Chem.* **2001**, *1*, 189.